

# Transition between different coherent light–matter interaction regimes analyzed by phase-resolved pulse propagation

Tilman Höner zu Siederdissen, Nils C. Nielsen, and Jürgen Kuhl  
*Max-Planck-Institut für Festkörperforschung, 70569 Stuttgart, Germany*

Martin Schaarschmidt, Jens Förstner, and Andreas Knorr  
*Institut für Theoretische Physik, Technische Universität Berlin, 10623 Berlin, Germany*

Galina Khitrova and Hyatt M. Gibbs  
*Optical Sciences Center, University of Arizona, Tucson, Arizona 85721*

Stephan W. Koch  
*Department of Physics and Material Sciences Center, Philipps-Universität, 35032 Marburg, Germany*

Harald Giessen  
*4th Physics Institute, University of Stuttgart, 70569 Stuttgart, Germany*

Received January 19, 2005

We present phase-resolved pulse propagation measurements that allow us to fully describe the transition between several light–matter interaction regimes. The complete range from linear excitation to the breakdown of the photonic bandgap on to self-induced transmission and self-phase modulation is studied on a high-quality multiple-quantum-well Bragg structure. An improved fast-scanning cross-correlation frequency-resolved optical gating setup is applied to retrieve the pulse phase with an excellent signal-to-noise ratio. Calculations using the semiconductor Maxwell–Bloch equations show qualitative agreement with the experimental findings. © 2005 Optical Society of America  
*OCIS codes:* 190.5530, 190.5970.

Interaction of propagating ultrashort laser pulses with solid-state materials is of major scientific and technical interest. To obtain a complete understanding of pulse modifications induced by the material, it is crucial to determine not only the field intensity but also the phase.<sup>1</sup> This phase information is vital to identifying output pulse properties such as chirp or relations between split-off pulse components, e.g., phase jumps. In the vicinity of an optical resonance in a semiconductor (SC) the Kerr model does not provide an adequate description of the nonlinearity.<sup>2</sup> Thus, if the nonlinear refractive index is undetermined or if the dipole matrix element of the transition itself is unknown, it is often difficult to unambiguously attribute a temporal pulse breakup after propagation to a certain physical mechanism. So far, most experiments in SC optics have neglected the phase. Recent experiments<sup>3–5</sup> have clearly shown that knowledge of the phase gives new insight into different light–matter interaction regimes, such as polariton beating in bulk SCs, self-induced transmission in SCs, and self-phase modulation (SPM) soliton formation in optical fibers. It must be emphasized though that each of these effects has been studied in a completely different material system until now.

In this Letter we provide a comprehensive study of the transition between these fundamental light–matter interaction regimes in one single material system. It is the phase information that allows us to

clearly identify the involved linear and nonlinear effects. We present phase-resolved subpicosecond pulse propagation measurements based on a fast-scanning cross-correlation frequency-resolved optical gating<sup>6</sup> (XFROG) setup. We thereby achieve an excellent signal-to-noise ratio and low retrieval errors of the XFROG algorithm. We compare our experimental findings with calculations that use the SC Maxwell–Bloch equations. As a suitable material system, we chose an (In,Ga)As/GaAs multiple-quantum-well (MQW) Bragg structure, which is a one-dimensional resonant photonic crystal. Our studies cover the complete intensity range from linear propagation to the breakdown of the photonic bandgap<sup>7</sup> (PBG) owing to increasing nonlinear excitation on to self-induced transmission<sup>8,9</sup> and up to the strong SPM regime.<sup>10</sup> We include investigations at substantially higher intensities than previous publications on MQW Bragg structures<sup>9</sup> and soliton formation.<sup>5</sup>

The sample we used was epitaxially grown on a 450- $\mu\text{m}$ -thick GaAs wafer and consists of 60  $\text{In}_{0.04}\text{Ga}_{0.96}\text{As}$  quantum wells (QWs) with a thickness of 8.5 nm separated by GaAs barriers. The barrier thickness monotonically increases from one side of the sample to the other. In this way we can adjust interwell distance  $d$  by changing the position of the laser excitation spot. For exciton resonance  $\lambda_{\text{ex}} = 830$  nm and refractive index  $n \approx 3.65$  of the GaAs

barrier material the Bragg resonance is achieved for  $d \approx 113.7$  nm. The front surface was coated with an antireflection layer. Linear reflection and extinction data of this sample (DBR17) can be found in Ref. 9.

Our experimental setup is shown in Fig. 1. The mode-locked 100-fs pulse train from a Ti:sapphire oscillator—tuned to the heavy-hole 1s exciton resonance at 830 nm and operating at 76 MHz—is split 2:1. The strong part is directed into a pulse shaper to tailor 580-fs pulses with a  $\text{sech}^2$  intensity profile spectrally matched to the resonance. It is focused onto the sample with an  $f=25$  mm microscope objective. The other part enters a variable delay line. The MQW sample is kept at 10 K in a cold-finger cryostat. The beam transmitted through the sample is superimposed with the delayed reference pulse in a  $\beta$ -barium borate crystal. The resulting sum-frequency signal is dispersed in a spectrometer and recorded by a CCD camera. In front of the spectrometer we placed a galvanometric scanning mirror that periodically modulates the vertical beam position on the CCD array. This modulation is synchronized to the shaker in the delay line. The signal is recorded as a function of delay and wavelength resulting in a XFROG trace averaged at 60 Hz. The XFROG retrieval algorithm<sup>6</sup> yields the time-dependent intensity and phase of the electric field.

Figure 2 shows our results for different input intensities. Thin and thick curves represent the normalized intensity and phase of the electric field versus time, respectively. The corresponding normalized spectra are shown in Fig. 3. The input pulse [Fig. 2(a)] exhibits a nearly constant phase over the pulse with slightly chirped outer wings. Because of the dispersion around the PBG, propagation at  $0.2$  MW/cm<sup>2</sup> results in two distinct pulse components with different carrier frequencies, i.e., linear phase segments with different slopes in the time domain<sup>1</sup> [Fig. 2(b)] and two peaks in the spectral domain [Fig. 3(b)], respectively. The temporal phase jump of  $\pi$  between the split-off pulse components clearly confirms a propagation beating.<sup>9</sup> The exciton resonance is broadened by the superradiant coupling and forms a PBG that leaves two spectral wings from the input spectrum. The two spectral components transform into a temporal beating with  $\pi$  phase shifts between the pulse components. However, only one beat period is found, owing to the rapid radiative dephasing ( $T_2 \approx 400$  fs).<sup>9</sup> Increasing the input intensity results in suppression of the beating [Fig. 2(c)] and increased transmission at the exciton resonance [Fig. 3(c)]. The phase jump disappears and evolves into a steeply

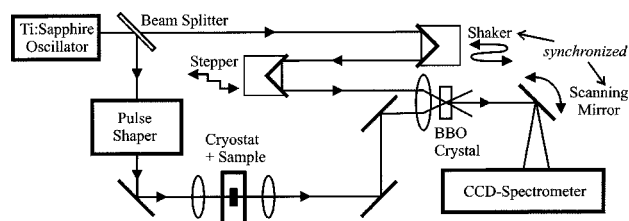


Fig. 1. Fast-scanning XFROG setup (BBO,  $\beta$ -barium borate).

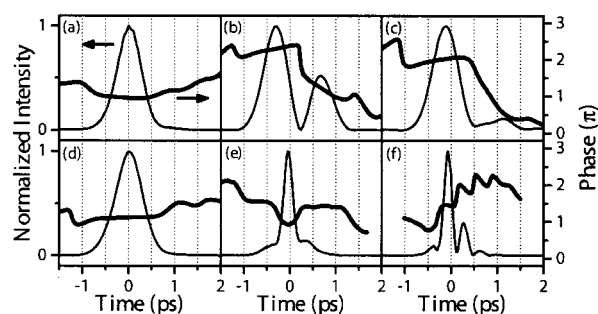


Fig. 2. Experimental XFROG results: Normalized intensity (thin curve) and phase (thick curve) versus time of the (a) input and (b)–(f) output pulses for input intensities of (b)  $0.2$ , (c)  $2.5$ , (d)  $15$ , (e)  $110$ , and (f)  $580$  MW/cm<sup>2</sup>.

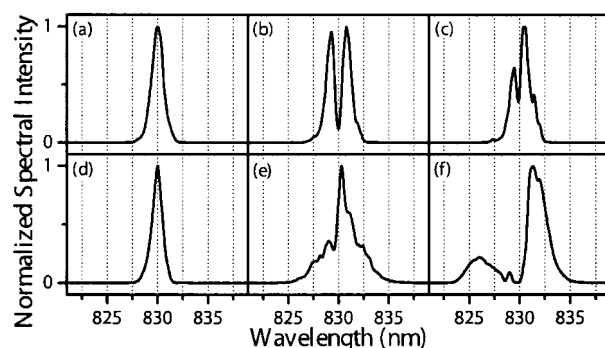


Fig. 3. Retrieved spectra corresponding to Fig. 2 of the (a) input and (b)–(f) output pulses for input intensities of (b)  $0.2$ , (c)  $2.5$ , (d)  $15$ , (e)  $110$ , and (f)  $580$  MW/cm<sup>2</sup>.

falling phase. This reflects the breakdown of the superradiant mode owing to the Pauli-blocking nonlinearity and the adiabatically driven electron dynamics<sup>7,9</sup> that gradually decouple the QW polarization from the light field for the time of the pulse duration. At  $15$  MW/cm<sup>2</sup> the output pulse with a flat phase leaves the sample essentially unaltered [Fig. 2(d)], presuming we neglect a decrease in pulse energy and a slight broadening induced by the dispersion of the  $450$ - $\mu\text{m}$  bulk substrate. The spectrum does not differ noticeably from the input spectrum. This phenomenon of self-induced transmission in SCs<sup>8,9</sup> indicates that a full Rabi flop of the carrier density has occurred within the suppressed bandgap of the MQW structure. Further increase of the intensity leads to SPM, which is immediately evident in spectral wings [Fig. 3(e)]. This initially forms a well-shaped phase around the main pulse [Fig. 2(e)], i.e., a steep phase at both sides of the main pulse (analogous to propagation in fibers<sup>5</sup> with switched signs of dispersion and Kerr nonlinearity). At even higher input intensities the spectrum is split into two components by strong SPM [Fig. 3(f)], and the pulse develops into a temporal pulse train [Fig. 2(f)]. The intensity of the spectral component closer to the band edge (smaller wavelengths) is lower because of reabsorption. The initial laser spectrum is strongly suppressed, i.e., converted into new frequency components. The separation between peaks of approximately  $10$  meV ( $\Delta t \approx 400$  fs) corresponds to the temporal beating period of  $350$  fs. Small phase

jumps ( $\approx \pi/2$ ) can be seen between the subsequent pulses. Experiments in bulk GaAs show the same pulse breakup but with full  $\pi$  phase jumps (not shown here). This indicates that in this regime the bulk effect of the substrate clearly dominates while a zero crossing of the field (necessary for a full  $\pi$  phase jump) is prevented by the nonlinearly excited QWs. The main pulse in Fig. 2(f) has a flat phase, indicating solitonlike propagation. The excess energy forms the adjacent pulses, which are too weak to compensate the dispersion and are therefore chirped. A beating induced by the interplay of dispersion and nonlinearity has been called modulational instability in the literature,<sup>11</sup> whereas the phase behavior suggests SPM beating. Measurements with an interwell distance detuned from the Bragg condition show more beating periods for linear excitation owing to the increased dephasing time of several picoseconds. However, in the nonlinear regimes in which the QW polarization is decoupled from the light field, there is no significant difference from the Bragg-resonant case.

The theoretical description of the light propagation effects requires splitting the sample into a MQW structure and bulk wafer. For resonant propagation in the MQW we calculate the transmitted signal by numerically solving the SC Maxwell–Bloch equations in the Hartree–Fock limit<sup>12</sup> using the finite-difference time-domain method.<sup>7,13</sup> This method allows the calculation of multiple reflection, backreflection, and light propagation in both directions and reproduces the formation and suppression of the PBG as shown in Ref. 7. For the subsequent off-resonant propagation through the bulk SC below the excitonic resonance, Maxwell’s equations are evaluated with the slowly varying envelope approximation.<sup>14,15</sup> The source terms in Maxwell’s equations for bulk propagation are calculated with the first excitonic resonance (which is sufficient for off-resonant excitation).<sup>10</sup> This approach allows us to reproduce the observed SPM and soliton formation [Fig. 2]. In this model the SPM is caused by escape from adiabatic following.<sup>10</sup> The numerical parameters are standard GaAs parameters. Plane waves propagating perpendicularly to the QWs are assumed. The effective propagation length and intensity are coupled parameters in our model that need to be adjusted to achieve good agreement. Therefore we set the effective length to 300  $\mu\text{m}$  and reduced the peak pulse intensities. We attribute this necessity to the neglect of transverse effects such as a defocusing nonlinearity. The main experimental features are well reproduced by our calculations [Fig. 4]. All the phase jumps occur as expected, although the SPM beating is less pronounced. The exact temporal variation of the phase depends sensitively on the pulse parameters chosen. The phase evolution in Fig. 4(d) and that of the input pulse differ by a linear phase term, i.e., a slight spectral shift. The measured spectra are well reproduced by numerically calculated spectra (not shown here).

In conclusion, we have presented phase-resolved pulse propagation measurements and numerical calculations of the transition between different light–matter interaction regimes in one single SC MQW

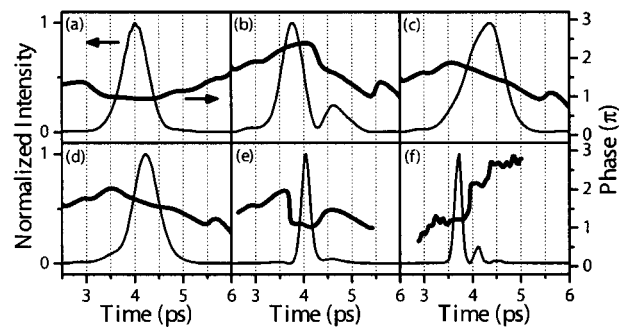


Fig. 4. Numerical calculations corresponding to Fig. 2 for input pulse areas of (a) input, (b)  $0.01 \pi$ , (c)  $1.6 \pi$ , (d)  $1.8 \pi$ , (e)  $2.3 \pi$ , and (f)  $4 \pi$ .

Bragg structure. Various regimes, such as linear propagation, breakdown of the PBG, and self-induced transmission, were covered. At the highest applied intensities, a SPM-induced beating has been demonstrated.

We thank the Deutsche Forschungsgemeinschaft (SFB296, SPP1113, and FOR557) and the Bundesministerium für Bildung und Forschung (FKZ13N8340/1) for support. T. Höner zu Siederdisen’s e-mail address is t.hoener@fkf.mpg.de.

## References

1. R. Trebino, *Frequency-Resolved Optical Gating: The Measurement of Ultrashort Laser Pulses* (Kluwer Academic, Boston, Mass., 2002).
2. T. Meier, S. W. Koch, P. Brick, C. Ell, G. Khitrova, and H. M. Gibbs, *Phys. Rev. B* **62**, 4218 (2000).
3. J. S. Nägerl, B. Stabenau, G. Böhne, S. Dreher, R. G. Ulbrich, G. Manzke, and K. Henneberger, *Phys. Rev. B* **63**, 235202 (2001).
4. N. C. Nielsen, T. Höner zu Siederdisen, J. Kuhl, M. Schaarschmidt, J. Förstner, A. Knorr, and H. Giessen, *Phys. Rev. Lett.* **94**, 057406 (2005).
5. F. G. Omenetto, B. P. Luce, D. Yarotski, and A. J. Taylor, *Opt. Lett.* **24**, 1392 (1999).
6. S. Linden, H. Giessen, and J. Kuhl, *Phys. Status Solidi B* **206**, 119 (1998).
7. M. Schaarschmidt, J. Förstner, A. Knorr, J. P. Prineas, N. C. Nielsen, J. Kuhl, G. Khitrova, H. M. Gibbs, H. Giessen, and S. W. Koch, *Phys. Rev. B* **70**, 233302 (2004).
8. H. Giessen, A. Knorr, S. Haas, S. W. Koch, S. Linden, J. Kuhl, M. Hetterich, M. Grün, and C. Klingshirn, *Phys. Rev. Lett.* **81**, 4260 (1998).
9. N. C. Nielsen, J. Kuhl, M. Schaarschmidt, J. Förstner, A. Knorr, S. W. Koch, G. Khitrova, H. M. Gibbs, and H. Giessen, *Phys. Rev. B* **70**, 075306 (2004).
10. P. A. Harten, A. Knorr, J. P. Sokoloff, F. B. Decolstoun, S. G. Lee, R. Jin, E. M. Wright, G. Khitrova, H. M. Gibbs, S. W. Koch, and N. Peyghambarian, *Phys. Rev. Lett.* **69**, 852 (1992).
11. K. Tai, S. Hasegawa, and A. Tomita, *Phys. Rev. Lett.* **56**, 135 (1986).
12. M. Lindberg and S. W. Koch, *Phys. Rev. B* **38**, 3342 (1988).
13. K. Yee, *IEEE Trans. Antennas Propag.* **14**, 302 (1966).
14. L. Allen and J. H. Eberly, *Optical Resonance and Two-Level Atoms* (Wiley, New York, 1975).
15. A. Knorr, R. Binder, M. Lindberg, and S. W. Koch, *Phys. Rev. A* **46**, 7179 (1992).